



RESEARCH ARTICLE

10.1029/2018EF001094

Impacts of Sulfate Geoengineering on Rice Yield in China: Results From a Multimodel EnsemblePei Zhan^{1,2} , Wenquan Zhu^{1,2} , Tianyi Zhang³, Xuefeng Cui⁴, and Nan Li²**Key Points:**

- G4 sulfate geoengineering is projected to increase irrigated rice yield in China by $5.3 \pm 5.7\%$
- G4 sulfate geoengineering is projected to increase rainfed rice yield in China by $4.8 \pm 7.3\%$
- Temperature is the dominant factor driving the rice yield changes

Supporting Information:

- Supporting information S1

Correspondence to:W. Zhu,
zhuwq75@bnu.edu.cn**Citation:**Zhan, P., Zhu, W., Zhang, T., Cui, X., & Li, N. (2019). Impacts of sulfate geoengineering on rice yield in China: Results from a multimodel ensemble. *Earth's Future*, 7, 395–410. <https://doi.org/10.1029/2018EF001094>

Received 7 NOV 2018

Accepted 17 MAR 2019

Accepted article online 22 MAR 2019

Published online 9 APR 2019

¹State Key Laboratory of Earth Surface Processes and Resource Ecology, Beijing Normal University, Beijing, China,²Beijing Engineering Research Center for Global Land Remote Sensing Products, Institute of Remote Sensing Science and Engineering, Faculty of Geographical Science, Beijing Normal University, Beijing, China, ³State Key Laboratory of Atmospheric Boundary Layer Physics and Atmospheric Chemistry, Institute of Atmospheric Physics, Chinese Academy of Sciences, Beijing, China, ⁴School of Systems Science, Beijing Normal University, Beijing, China

Abstract Sulfate geoengineering could mitigate global warming via injecting SO₂ into the stratosphere. However, its impacts on regional climate might lead to adverse consequences for local agriculture. In this study, we simulated the impacts of sulfate geoengineering on rice yield in China both with sufficient irrigation (irrigated) and without irrigation (rainfed). We used Geoengineering Model Intercomparison Project G4 climates from six climate models to force the ORYZA version 3 crop model to simulate rice yields under sulfate geoengineering scenario. G4 prescribes a sulfate injection to offset the radiative forcing in the Representative Concentration Pathway (RCP) 4.5 scenario. Results indicated that during the last 15 years of G4 sulfate geoengineering (i.e., 2055–2069), the implementation of sulfate geoengineering increases rice yields in most areas in China comparing with that without the implementation of sulfate geoengineering (i.e., RCP4.5), with a yield increase of $5.3 \pm 5.7\%$ for irrigated yield and $4.8 \pm 7.3\%$ for rainfed yield. After the termination of sulfate geoengineering, the irrigated rice yield in G4 is still significantly higher than that in RCP4.5, but such increase is not significant for rainfed yield. Temperature is always the dominant factor that drives the rice yield change no matter under irrigated or rainfed conditions, but the effect from solar radiation cannot be ignored in southern China.

1. Introduction

As a result of greenhouse gas emissions caused by anthropogenic activities, global warming has received widespread attention. The global average temperature has increased by 0.85 °C from 1880 to 2012, and it is projected to continue to increase to be at least 1.5 °C above the preindustrial level by the end of the 21st century (Stocker et al., 2013). Global warming is considered to have significant and far-reaching direct impacts on a global scale, such as increasing the frequency of extreme weather events (Allan & Soden, 2008; Fischer & Knutti, 2015) and raising sea levels (Alley et al., 2005; Gregory et al., 2004). Besides, global warming can indirectly affect society, the economy, and agriculture (McCarty, 2001; Patz et al., 2005; Piao et al., 2010; Rosenzweig & Parry, 1994; Walther et al., 2002) and ultimately affect the survival and development of human beings. Therefore, methods that aim to counter global warming have been widely discussed, and geoengineering is one of them (Marchetti, 1977).

Geoengineering is defined as the intentional large-scale manipulation of environment against global warming (Keith, 2000). There are many proposed schemes of geoengineering, among which sulfate geoengineering is one of the most discussed remedies for its low cost and feasibility (Lenton & Vaughan, 2009; Robock et al., 2009). With SO₂ continuously injected into the stratosphere, sulfate geoengineering can balance the radiative forcing caused by anthropogenic activities and achieve the preset goal of cooling (Crutzen, 2006). However, sulfate geoengineering may bring about a series of complex ripple effects (such as ozone depletion and regional precipitation reduction) that have potentially significant impacts on the climate system and socioeconomic aspects while cooling the Earth (Robock et al., 2008; Robock et al., 2009). Furthermore, through its impacts on temperature, radiation, and hydrology, especially the impacts on regional climate factors, the implementation of sulfate geoengineering may also affect the growth of crops and thus affect the final crop production and food security.

Some researchers have conducted studies on the impacts of geoengineering on agriculture. Pongratz et al. (2012) used a statistical model to evaluate the effects of the implementation of sulfate geoengineering on

©2019. The Authors.

This is an open access article under the terms of the Creative Commons Attribution-NonCommercial-NoDerivs License, which permits use and distribution in any medium, provided the original work is properly cited, the use is non-commercial and no modifications or adaptations are made.

global wheat, maize, and rice under a $2 \times \text{CO}_2$ scenario; the results showed that the yields of the three crops increase after the implementation of sulfate geoengineering except for rice at high latitudes. Although the statistical model requires less for model parameters and thus is easy to apply, it does not take into account the nonclimate factors of the crop cultivation (e.g., soil type and irrigation), and thus, the spatial variability of crop growth environment and management practices are ignored (Matala et al., 2003). Xia et al. (2014) applied the Decision Support System for Agrotechnology Transfer crop model to simulate the impacts of G2 geoengineering (solar diming) on rainfed rice and maize in China, and it was found that the implementation of geoengineering leads to an increase in maize production and a mild change in rice production in China as compared to without geoengineering, and the termination of geoengineering results in a great reduction in maize production. They also concluded that the precipitations are the most significant factors affecting these production changes of rainfed crops. Parkes et al. (2015) used the General Large Area Model to simulate the impacts of marine cloud brightening on crop failure rates of winter wheat in Northeastern China and groundnut in West Africa, and their results indicated that increased rainfall can reduce the numbers of crop failure rates in both regions. A key problem with previous studies regarding the impacts of geoengineering on rice in China is how they took into account the effect of precipitation (Pongratz et al., 2012; Xia et al., 2014), and Xia et al. (2014) even turned off the irrigation function in the simulation of rice yield (which means the only water resource for the growth of rice is from precipitation). However, almost all the rice planting areas in China are equipped with irrigation (Maclean et al., 2013). The turnoff of the irrigation function may lead to unreliable simulations in most parts of China, particularly those in the relatively arid area in the north of China. Therefore, when studying rice yield under future conditions, both rice yield with sufficient irrigation (irrigated) and without irrigation (rainfed) should be taken into consideration to provide a more comprehensive result.

The aim of this study is to evaluate the impacts of sulfate geoengineering on the temporal and spatial distribution of rice yield in China and to further quantify the effects of changes in each climate factor on rice yield under the sulfate geoengineering scenario. In this study, the Geoengineering Model Intercomparison Project (GeoMIP) G4 scenario was chosen as the sulfate geoengineering scenario. The historical observations from 318 meteorological stations in China and anomalies between the G4, Representative Concentration Pathway (RCP) 4.5 (the baseline of G4) and Historical scenarios from a multimodel ensemble were combined and input into the progress-based crop model ORYZA version 3 (v3) to simulate the rice yields in China under the G4 and RCP4.5 scenarios, and the impacts of sulfate geoengineering were studied by comparing the differences between the two yields. The differences between this study and previous works are (1) the G4 scenario in GeoMIP was chosen to study the impacts of sulfate geoengineering on rice yield in China, which can potentially provide supports for future decision-making, and (2) both irrigated and rainfed conditions were considered in the future rice yield simulation, thus giving a more comprehensive result.

2. Data and Methods

2.1. Observation Data

The regionalization map of rice planting in China and distribution of 318 meteorological stations were derived from T. Zhang et al. (2014). They matched the county-level rice yields with meteorological stations, screening out stations with less than 10 years of rice yield records, and finally, a total of 318 stations which are located near the rice planting area was derived for rice yield simulation. These stations cover 7 rice-planting subregions and 26 provinces, encompassing the main rice-planting area in China (Figure 1).

Rice trial data for this study were collected from the Agrometeorological Experiment Stations operated by the China Meteorological Administration. The data include cultivar data, critical phenological dates (emergence, transplanting, panicle initiation, flowering, and physiological maturity dates) of rice, yields, and management practices. The data were used as the inputs of cultivars and management practices for the crop model. The observation data from 318 meteorological stations were provided by the China Meteorological Data Service Center (<http://data.cma.cn/>); the observations include the daily maximum and minimum air temperature, precipitation, sunshine hour, relative humidity, wind speed, and so on. In this study, observations during 1976–2005 were chosen to generate the climate input for the crop model, in which sunshine hour was converted into solar radiation according to Ångström formula (Ångström, 1924). This method is also adopted by the crop model ORYZA(v3) to convert sunshine hour into solar

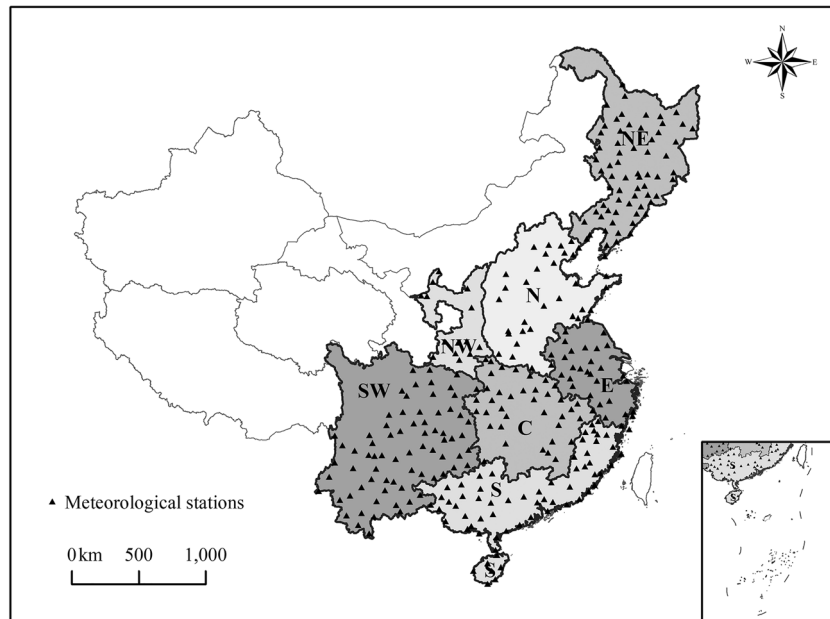


Figure 1. Study area and meteorological stations. The regionalization map of rice planting was from T. Zhang et al. (2014), and the main rice-planting area in China was divided into seven subregions, that is, single cropping area in the subhumid northeastern (NE), semiarid northern (N) and arid northwestern (NW) regions, single and double cropping area in the subhumid eastern (E), central (C), and southwestern (SW) regions, and double cropping area in humid southern (S) region.

radiation before its simulation. Relative humidity and temperature were converted into vapor pressure using equation (1) to meet the crop model input requirements. The temperature was first converted into saturated vapor pressure using Magnus-Tetens formula (Murray, 1967), and then vapor pressure was calculated using saturated vapor pressure and relative humidity.

$$VP = 0.61078 \times 10^{\left(\frac{7.5 \times T}{237.3 + T} + 0.7858\right)} \times \frac{RH}{100}, \quad (1)$$

where VP is the vapor pressure; T is the temperature in Celsius degree, here we used the average of the daily maximum and minimum temperatures; and RH is the relative humidity.

2.2. Climate Scenario Data

We chose G4 scenario from GeoMIP as the sulfate geoengineering scenario. In the design of the G4 scenario, SO_2 is injected into the stratosphere at a rate of 5 Tg/year to offset the radiative forcing in the RCP4.5 scenario (stabilized at 4.5 W/m^2 above the preindustrial level in the year 2100). The experiment of sulfate geoengineering is set to start in 2020 and lasts for 50 years. At 2070, the injection of SO_2 will be stopped, and an additional 20-year simulation is added to study the response to the cessation of sulfate geoengineering or termination effect (Kravitz et al., 2011).

In this study, we used daily simulations from six climate models to generate the climate inputs for the crop model (Table 1). Climate simulations of RCP4.5 were used to represent a global warming scenario, simulations of G4 were used to represent a scenario where sulfate geoengineering is implemented under the background of global warming, and simulations of Historical were used to represent the historical climate change. For each climate model, if there were more than one ensemble members, then each ensemble member was processed separately for crop model simulation.

The climate factors in consideration are daily maximum and minimum air temperature, solar radiation, precipitation, wind speed, and relative humidity, in which relative humidity and temperatures were also converted into vapor pressure using equation (1).

Table 1
Information of the Six Contributing Climate Models

Model	Spatial resolution of the atmospheric model (number of grid cells: longitude × latitude)	Ensemble members (G4/RCP4.5/Historical)	References
BNU-ESM	128 × 64	1/1/1	Ji et al. (2014)
CanESM2	128 × 64	3/3/3	Chylek et al. (2011)
CSIRO-Mk3L-1-2	64 × 56	3/3/3	Phipps et al. (2011)
HadGEM2-ES	192 × 145	1/1/1	Collins et al. (2011)
MIROC-ESM	128 × 64	1/1/1	Watanabe et al. (2011)
MIROC-ESM-CHEM	128 × 64	1/1/1	Watanabe et al. (2011)

2.3. Crop Model

The ORYZA(v3) model was used to simulate the response of rice growth and yield to climate change. The ORYZA model series are progress-based crop models developed by International Rice Research Institute. They can simulate the growth, development, and finally the yield of rice. The simulating accuracy of ORYZA2000 for the growth, phenology, and yield of rice has been validated in various regions over the world (Yadav et al., 2011; Zhang et al., 2014) and under different management practices (Bouman & van Laar, 2006; Marcaida et al., 2014). As for the advanced version of ORYZA2000, ORYZA(v3) has advanced the quantitative assessment of the effects of drought, nitrogen deficiency, and different irrigation practices on the basis of the ORYZA2000 model (Li et al., 2017). After inputting the climate data, crop management data, and crop attribute data required, the model can simulate the growth of rice and, hence, the yield.

The calibration and validation of the ORYZA model for its application in China has been done in our previous work (Zhang et al., 2014), in which the normalized root-mean-square error was approximately 15% and 5% for the yield and phenological dates, respectively. In this study, the simulation of rice yield in China was performed on the basis of the calibrated ORYZA model. In this study, both rice yield with sufficient irrigation (irrigated) and without irrigation (rainfed) were taken into consideration for a more robust result. As for fertilization considerations, we only considered fertilization effects from CO₂, while other fertilizers (such as N fertilizers) were not considered because the lack of data. In this study, CO₂ concentration was set for each year according to the global average CO₂ concentration data of RCP4.5 scenario provided by Meinshausen et al. (2011) to simulate rice yield. Since different cultivars response differently to the climate change, different rice cultivars were set for different provinces in this study in order to reflect the rice cultivation in China more precisely (Table 2). Because of the lack of the observed diffuse radiation data, the changes in diffuse radiation was also not considered in this study.

2.4. Rice Yield Simulation Under the Impacts of Sulfate Geoengineering

Considering the differences in planting structure, cultivation, and climate in different regions in China, the raw outputs from climate models may not precisely reflect the spatial difference of rice planting in China, hence a “delta” method was used to downscale the climate outputs from the climate models (Hawkins et al., 2013). The historical observations and Historical simulations were first converted into climatology by averaging the 30-year climate in each day. As for temperatures, two sets of daily anomalies (i.e., the anomaly between G4 and climatology of Historical scenario and the anomaly between RCP4.5 and climatology of Historical scenario) were added to the 30-year averaged daily historical climate observations in 318 stations. As for other climate variables, the daily change ratios between the two future scenarios and the climatology of Historical scenario were used as a multiplicative factor to obtain future climate conditions in the 318 stations (Figure 2). In this case, a climate model grid may contain several stations, so for each grid, the climate anomalies were added to all the stations within its spatial extent. Since a climate model may have several ensemble members, we first simulated the rice yield based on each ensemble member of each model, and then we used the average of all the ensemble member-based rice yield as the model-based rice yield.

In the design of GeoMIP, the G4 scenario is projected to start in 2020 and end in 2089, in which 2020–2069 is the period of sulfate geoengineering and 2070–2089 is the period after the termination of sulfate geoengineering. We followed Xia et al. (2014) to choose the period 2055–2084 to evaluate the impacts of sulfate

Table 2
Cultivars Used for Rice Yield Simulation in Each Province in China

Province	Cropping Season	Cultivar
Heilongjiang	Single	Kongyu-131
Jilin	Single	Qiuguang
Liaoning	Single	Liaojin294
Beijing	Single	Kendao95-4
Tianjin	Single	Kendao95-4
Hebei	Single	Kendao95-4
Henan	Single	Tesanai-2
Shandong	Single	Tesanai-2
Shanxi	Single	Kendao95-4
Shaanxi	Single	Ningjing-29
Ningxia	Single	Ningjing-29
Jiangsu	Single	Zaofeng-8
Anhui	Single	Xieyou-63
Zhejiang	Early	Zhe-733
Zhejiang	Late	Eryou-92
Hubei	Single	Shanyou-63
Hunan	Early	Zhefu-7
Hunan	Late	Yuchi231-8
Jiangxi	Early	Ganzaoxian-14
Jiangxi	Late	Zhongyougui-99
Sichuan	Single	Dyou-63
Chongqing	Single	Eryou-258
Yunnan	Single	Dianxi-15
Shanghai	Single	Zaofeng-8
Guizhou	Single	Jinyou-63
Fujian	Early	Jiayu-164
Fujian	Late	Kyou-17
Guangdong	Early	Zayou
Guangdong	Late	Guanger-104
Guangxi	Early	Teyou-63
Guangxi	Late	Boyou-903
Hainan	Early	Teyou-63
Hainan	Late	Boyou-903

geoengineering on rice in China. The period is composed of two important phases. (1) The last 15 years of sulfate geoengineering (i.e., 2055–2069, hereinafter referred to as the geoengineering phase), this period has the strongest climate signal of geoengineering. (2) The 15 years after the termination of sulfate geoengineering (i.e., 2070–2084, hereinafter referred to as the termination phase), this period was chosen to study the termination effect.

The downscaled climates representing G4 and RCP4.5 of each climate model were input into the crop model, and the differences between the G4 yields and the RCP4.5 yields can illustrate the impact of sulfate geoengineering on rice. On the purpose of studying the rice yield change in the future, both irrigated yield and rainfed yield were simulated.

2.5. Analysis of the Effect of Dominant Climate Factor on Rice Yield

A multiple linear regression (MLR) analysis was applied to determine the dominant climate factor that affects the rice yield change between the G4 yield and the RCP4.5 yield. The MLR uses the annual changes of the climate factors (maximum and minimum temperatures, solar radiation, precipitation, wind speed, and relative humidity) between G4 and RCP4.5 as independent variables and annual rice yield changes between G4 and RCP4.5 as the predictor. The MLR was done in terms of irrigated yields and rainfed yields; when irrigated yields were set as the predictor, the independent variables considered are only maximum temperature, minimum temperature, and solar radiation, because when irrigation function is turned off, the only impacting factors are these three factors. The MLR was done in each subregion and in the whole China. For each subregion, the climates and yields were averaged over all the stations within this subregion as the independent variables and predictor. In order to reduce the collinearity among different variables and eliminate the differences among the order of magnitude of different variables, each variable was first normalized through subtracting its mean and then divided by its standard deviation. The MLR model can be represented by equation (2).

$$Y = \beta_0 + \beta_1 X_1 + \beta_2 X_2 + \dots + \beta_n X_n + \epsilon, \quad (2)$$

where Y is the predictor (dependent variable), X_1 to X_n are the independent variables, β_1 to β_n are the coefficients relating the independent variables to the dependent variable, and ϵ is the residual error. A greater

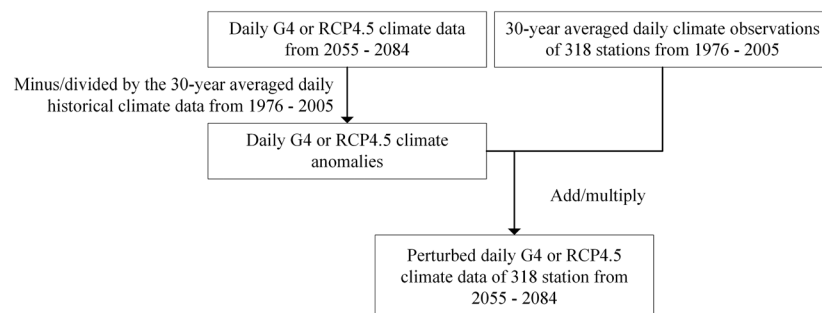


Figure 2. Production of the daily climate data under the G4 and RCP4.5 scenarios. The so-called “delta” method was used to combine the daily climate under the G4, RCP4.5, and Historical scenarios with the daily observations from 318 stations to produce the downscaled daily climate of G4 and RCP4.5 scenarios as the climate input of the ORYZA model. RCP = Representative Concentration Pathway.

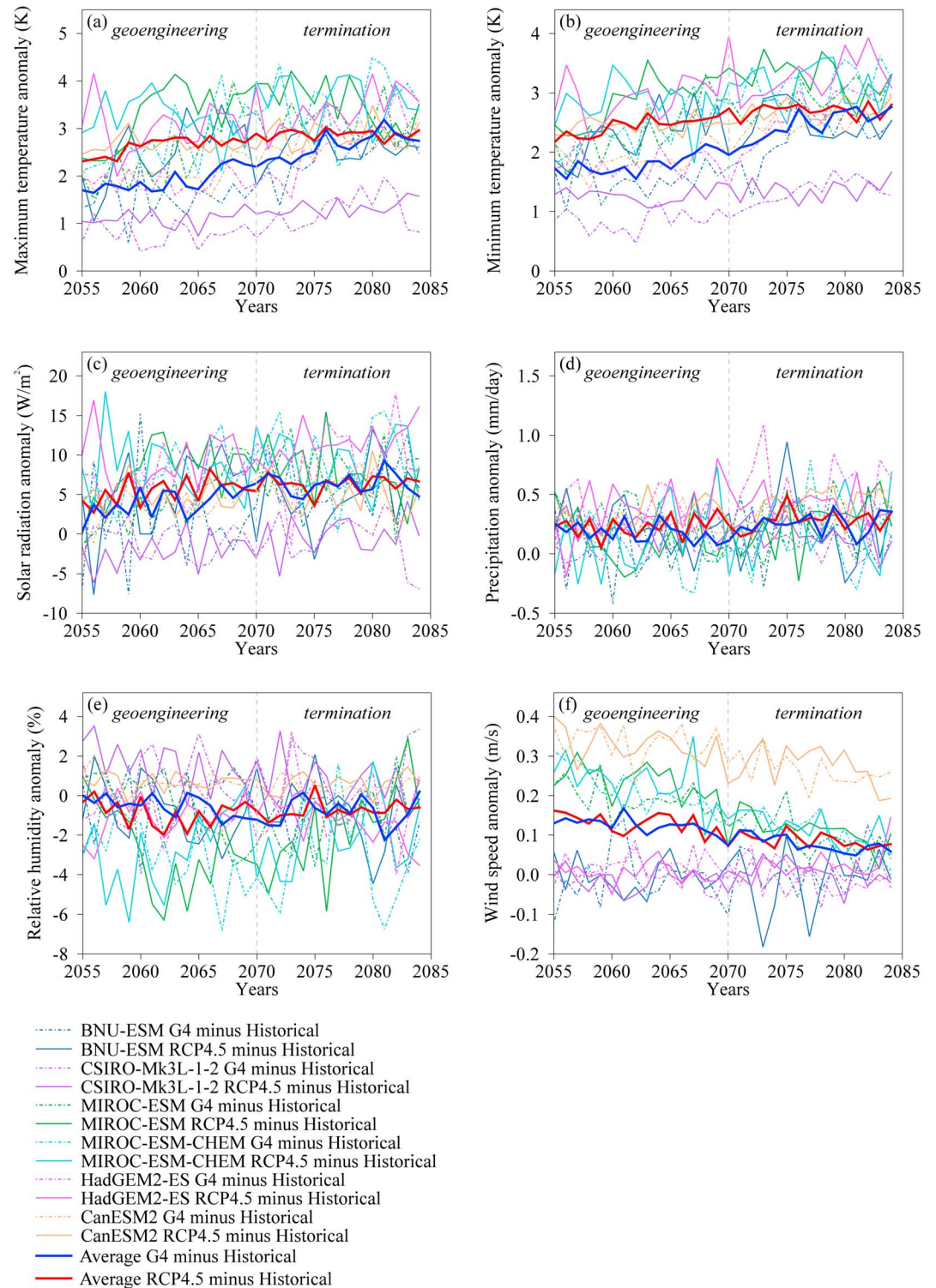


Figure 3. Annual average of the climate anomalies between the G4, RCP4.5, and Historical scenarios in rice cropping area in China. The results were from six climate models averaged over 318 stations. (a)–(f) are annual averages of the maximum temperature, minimum temperature, solar radiation, precipitation, relative humidity, and wind speed, respectively. The blue lines are climate anomalies between G4 and Historical (G4 minus Historical), and the red lines are climate anomalies between RCP4.5 and Historical (RCP4.5 minus Historical). The thick lines are the anomalies averaged over the six climate models, and the dashed lines are the climate anomalies of each climate model. RCP = Representative Concentration Pathway.

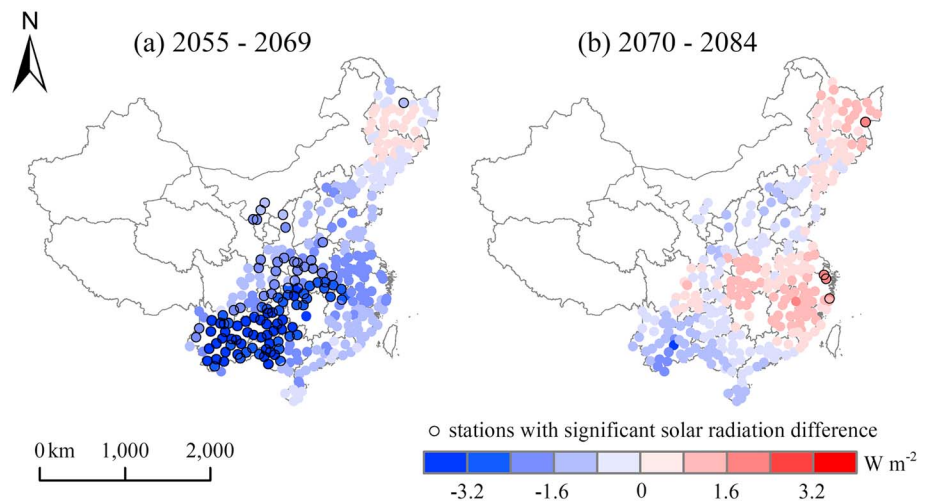


Figure 4. The multimodel averaged solar radiation difference between G4 and Representative Concentration Pathway 4.5 (G4 minus Representative Concentration Pathway 4.5) in each station during the geoengineering phase (a) and termination phase (b).

absolute value the coefficient of an independent variable has, the more this variable dominates the rice yield change. Furthermore, the coefficients were converted into percentages, which were used to measure the dependence of rice yield change on the climate variables.

2.6. Statistical Significance Test of the Climate/Rice Yield Changes

We tested the statistical significance of the difference between G4 and RCP4.5. A paired-by-two student's *t* test was conducted to test the statistical significance of the difference of interannual yield/climate changes between G4 and RCP4.5. A *p* value that is equal or less than 0.05 indicates a significant difference between the compared elements under the two scenarios.

3. Results

3.1. Climate Anomalies Under the Impacts of Sulfate Geoengineering

The implementation of sulfate geoengineering results in reducing approximate 1.7 W/m^2 of solar radiation in rice cropping area in China compared with that under the RCP4.5 scenario during the geoengineering phase (2055–2069; Figure 3c), achieving a cooling of about $0.8 \text{ }^\circ\text{C}$ in the average temperature (Figures 3a and 3b). The temperature reduction ranges from $0.29 \text{ }^\circ\text{C}$ in CSIRO-Mk3L-1-2 to $1.17 \text{ }^\circ\text{C}$ in HadGEM2-ES, and all of them are significant. The precipitation change is not significant during the geoengineering phase in the multimodel averaged result (Figure 3d). However, CSIRO-Mk3L-1-2 reported a significant precipitation reduction of 0.13 mm/day . After the termination of sulfate geoengineering, the temperature gap between G4 and RCP4.5 remains almost constant for nearly 6 years in the rice cropping area, and this gap was found significant in all climate models except for CanESM2 and MIROC-ESM-CHEM. As for termination effect, three models (BNU-ESM, CanESM2, and HadGEM2-ES) reported a clear quick warming in rice cropping area in China. After 2075, the temperature in G4 bounces back to the RCP4.5 level within 1 year (Figures 3a and 3b), and no significant difference between the temperatures under the two scenarios was found after 2075 except for that in HadGEM2-ES. As for precipitation, no significant change was found during the termination.

As for the spatial distribution of the climate change, the implementation of sulfate geoengineering results in a significant solar radiation reduction in the south of China in the G4 scenario compared with that in RCP4.5 (Figure 4), and this reduction is greater in the south areas than in the north. After the termination, almost all stations show no significant solar radiation change. However, the temperature changes in G4 relative to RCP4.5 are much more significant. The maximum and minimum temperatures in G4 are all significantly lower than those in RCP4.5 during the geoengineering phase, and these reductions in temperatures are still significant in northern China during the termination phase (Figure 5). However, the temperature reductions

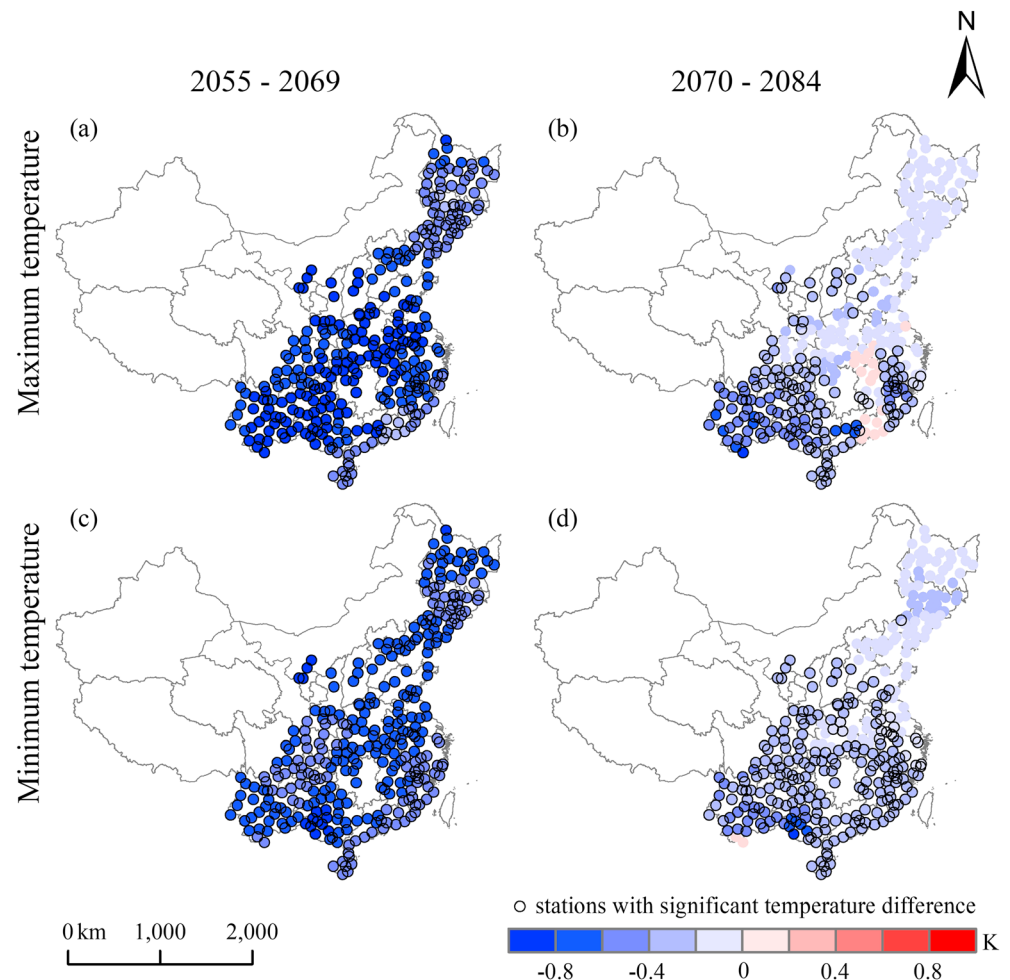


Figure 5. The multimodel averaged temperature difference between G4 and Representative Concentration Pathway 4.5 (G4 minus Representative Concentration Pathway 4.5) in each station. (a) Maximum temperature difference during the geoengineering phase, (b) maximum temperature difference during the termination phase, (c) minimum temperature difference during the geoengineering phase, and (d) minimum temperature difference during the termination phase.

are pervasively weakened after the termination of sulfate geoengineering. The precipitation change is not significant in most areas in China no matter during the geoengineering phase or the termination phase (Figure 6), but significant precipitation reduction can be found in northeastern China during the geoengineering phase and eastern China during the termination phase.

3.2. Impacts of Sulfate Geoengineering on Irrigated Rice Yield in China

During the geoengineering phase, the averaged irrigated rice yield in China in G4 is always significantly higher than that in RCP4.5 (Figure 7a), and all the six models show a significant positive rice yield change in G4 compared to RCP4.5 (ranging from $2.2 \pm 4.0\%$ for CSIRO-Mk3L-1-2 to $6.9 \pm 10.6\%$ for HadGEM2-ES, the values after plus/minus denote the 1 standard deviation of 318 stations; Figure 8a). After the termination of sulfate geoengineering, the averaged irrigated rice yield in G4 drops, but it maintains significantly higher than the RCP4.5 level for almost 10 years. After year 2080, the G4 yields are almost all within the natural variabilities (defined as 1 standard deviation of the interannual change of average yield in China during 2055–2084) of RCP4.5 yield. This changing pattern is similar to that of the temperature anomalies. During which period, all models exhibit smaller rice yield increase from RCP4.5 to G4 compared to that during geoengineering phase (Figure 8a). Here we define the irrigated rice yield simulated using the 30-year averaged climate during 1976–2005 as the irrigated rice yield at current level. It was found that

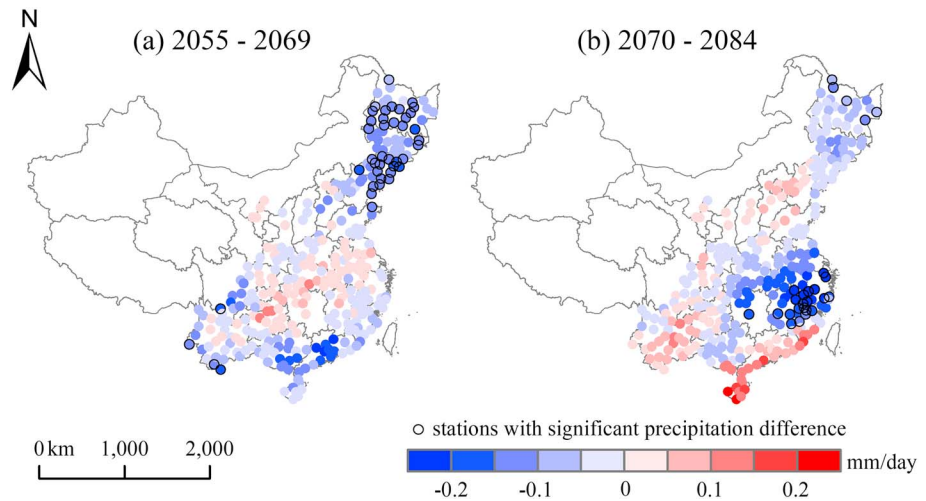


Figure 6. The multimodel averaged precipitation difference between G4 and Representative Concentration Pathway 4.5 (G4 minus Representative Concentration Pathway 4.5) in each station during the geoengineering phase (a) and termination phase (b).

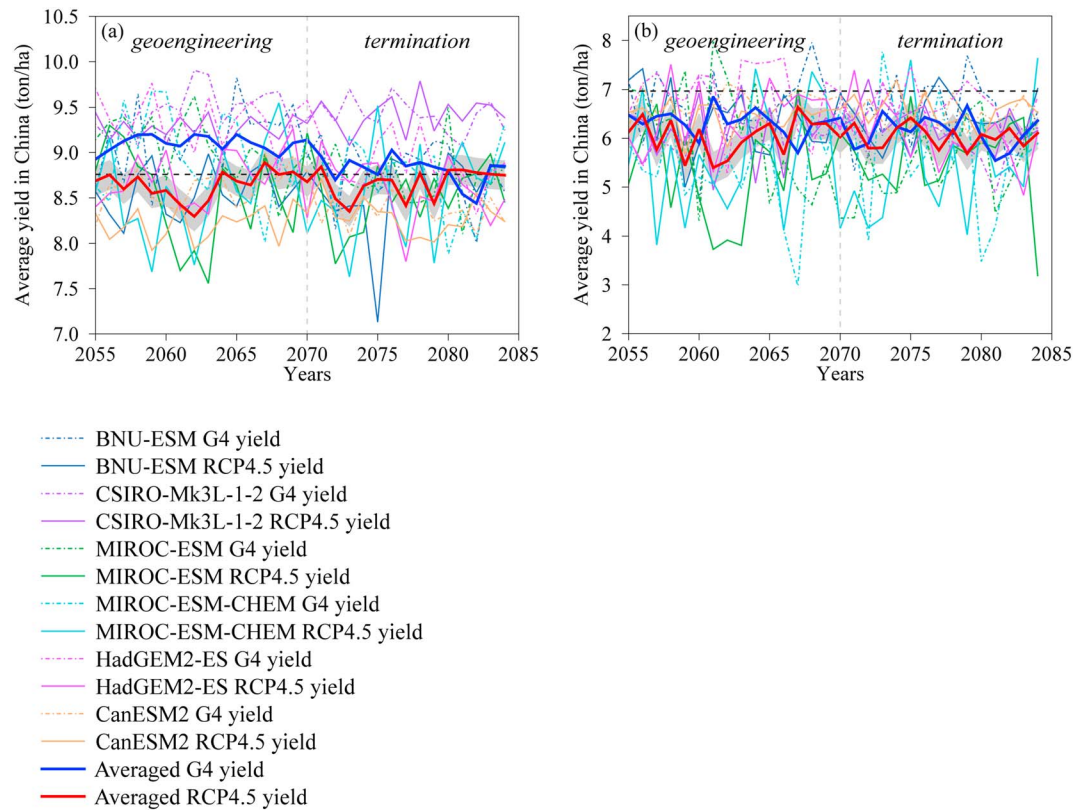


Figure 7. The interannual changes of the rice yield under the G4 and RCP4.5 scenarios averaged over 318 stations. The rice yields were simulated based on the climates from the six climate model outputs. (a) The interannual changes of the irrigated rice yield and (b) the interannual changes of the rainfed rice yield. The black dashed line is the rice yield under the averaged climate during 1976–2005. The gray area shows 1 standard deviation of the multimodel averaged RCP4.5 yield during 2055–2084, illustrating the effect of climate variability. RCP = Representative Concentration Pathway.

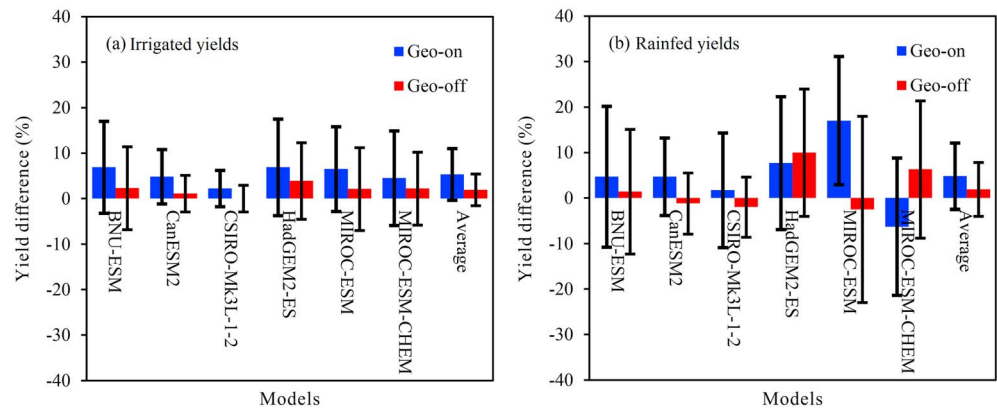


Figure 8. Average rice yield difference between G4 and Representative Concentration Pathway 4.5 (G4 minus Representative Concentration Pathway 4.5) in percentage of the six climate models. The error bars are 1 standard deviations of 318 stations during the geoengineering phase (geo-on) or termination phase (geo-off).

the average irrigated G4 yield during the geoengineering phase is significantly higher than the current yield level (3.9%), but the average irrigated RCP4.5 yield during 2055–2084 is a little lower (−1.3%, $p < 0.05$) than the current level.

Figure 9a shows the irrigated rice yield differences between G4 and RCP4.5 in the 318 stations averaged over the six climate models. During the geoengineering phase, there are 297 stations in G4 showing yield increases (ranging from 0.1% to 21.6%) compared with the yield in RCP4.5, and only 21 stations exhibit yield loss (ranging from −0.0% to −25.2%), which lead to a significant rice yield increase in G4 compared with RCP4.5 of $5.3 \pm 5.7\%$ (Figure 9a). When it comes to the spatial distribution of the yield change, yield increases are found statistically significant in all the seven subregions except for the northwestern region, among which the northeastern region has the most yield increase of $6.5 \pm 5.0\%$, followed by the central region of $6.3 \pm 5.0\%$, and only the yield increases in the northwestern ($0.5 \pm 9.9\%$) is relatively small (Table 3). Generally, the rice yield increase in the north part of China is a little higher than that in the southern areas. After the termination of sulfate geoengineering, the magnitudes of rice yield changes decrease, but the stations with increased rice yield still remains the majority (a total of 255 stations with yield increase ranging from 0.0% to 16.2%), leading to a significant yield increase of $1.9 \pm 3.5\%$ in G4 compared with RCP4.5 (Figure 9b), and similar yield increase was also found in all the seven subregions. However, the yield changes in most of the stations are not significant, which corresponds with the fact that the temperature and radiation in G4 pervasively increases after the termination of geoengineering. During this period, the northwestern region still has the weakest yield increase of $0.7 \pm 6.5\%$, and the rice yield increase is found only significant in the northeastern region of $2.9 \pm 2.9\%$ (Table 3).

3.3. Impacts of Sulfate Geoengineering on Rainfed Rice Yield in China

As for the rainfed rice yield in China, the implementation of sulfate geoengineering significantly increases yield by $4.8 \pm 7.3\%$ compared with the RCP4.5 level (Table 3). After the termination of sulfate geoengineering, the rice yield in G4 is still $1.9 \pm 5.9\%$ higher than that in RCP4.5 but not statistically significant, among which three models (CanESM2, CSIRO-Mk3L-1-2, and MIROC-ESM) even exhibit yield losses during this period but not significant (Figure 8b). Different from other models, MIROC-ESM-CHEM shows that the implementation of sulfate geoengineering results in a yield decrease for rainfed rice, but it is not statistically significant (Figure 8b). Unlike the changing pattern of the irrigated rice yield, the rainfed rice yield under the G4 scenario maintains significantly higher than the RCP4.5 yield only before 2066 (still within the geoengineering phase), and after 2066, the G4 yields are almost all within the natural variability of the RCP4.5 yields (Figure 7b).

During the geoengineering phase, similar to the changes of irrigated rice yields, a majority of stations (265 stations) show yield increases in G4 compared with the yields in RCP4.5 (ranging from 0.1% to 47.8%), and 53 stations show yield decreases (ranging from −0.2% to −26.2%; Figure 10a). However, the rice yield change patterns are much more scattered, the magnitudes of which are much higher

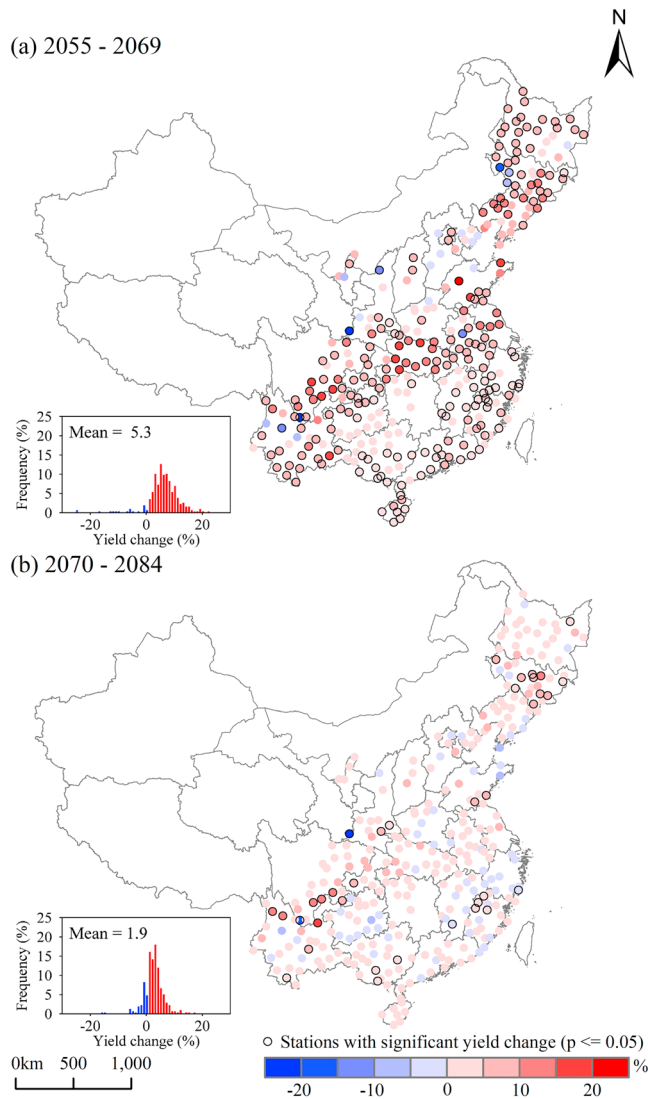


Figure 9. Irrigated rice yield differences in 318 stations between the G4 and Representative Concentration Pathway 4.5 (G4 minus Representative Concentration Pathway 4.5) scenarios averaged over the six climate models during the geoengineering phase (a) and the termination phase (b).

when compared with the irrigated yield changes, and less stations show significant yield change. During the geoengineering phase, rainfed yields in G4 are still higher than those in RCP4.5 in all the seven subregions but only significant in the northeastern and southern regions. Similar to the potential yield, the northeastern region has the greatest increase for rainfed yield of $8.8 \pm 6.8\%$, and the northwestern region has the most insignificant yield change ($1.7 \pm 11.9\%$). After the termination of sulfate geoengineering, about 30% of the stations show a yield loss in G4 compared with RCP4.5, and most of them are located in the north and central part of China (Figure 10b). As for each subregion, the rice yield in the northern region shows yield loss, and other subregions show yield increase, but the yield changes in all the subregions are insignificant.

3.4. Dependence of Rice Yield Changes on Each Climate Factors

Maximum temperature is the most dominant factor that affects the rice yield changes between G4 and RCP4.5 under sufficient water supply (irrigated yields), contributing to 53.6% of rice yield changes (Table 4). Spatially, maximum temperature dominates the rice yield changes in six subregions (except for the southern region). The changes in minimum temperature impact the rice yields more in the north part of China but not significant. As for solar radiation, greater impacts from solar radiation were found on rice yield changes in the southern areas (Table 4) but not significant. It is also worth noting that in some regions, the goodness of fitting of the MLR is quite low (such as northwestern), indicating that there may be some combined effect of climate variables or short-term weather change, which greatly affects the rice yield, not captured by the MLR analysis.

As for the rainfed rice yield, maximum temperature, minimum temperature, and solar radiation are the three variables with the greatest contribution to rice yield changes in the whole China. Similar to the irrigated yields, maximum temperature dominates the rice yield changes in China with a contribution rate of 41.3%, and solar radiation has some non-negligible impact on rice yield in southern China (Table 5). However, unlike the impacting pattern for the climates on the irrigated rice yields, the temperatures have greater impacts on the rainfed rice yields in the south of China but weaker impacts in central China. Precipitation is not

Table 3
Rice Yield Change Under G4 Comparing With That Under Representative Concentration Pathway 4.5 in the Seven Subregions

Region	G4 yield change (2055–2069)		G4 yield change (2070–2084)	
	Irrigated (%)	Rainfed (%)	Irrigated (%)	Rainfed (%)
NE	$6.5 \pm 5.0^{**}$	$8.8 \pm 6.8^*$	$2.9 \pm 2.9^*$	3.4 ± 6.4
N	$4.8 \pm 5.3^{**}$	3.3 ± 6.2	1.1 ± 2.7	-1.9 ± 6.6
NW	0.5 ± 9.9	1.7 ± 11.9	0.7 ± 6.5	0.4 ± 6.8
E	$5.8 \pm 5.0^{**}$	2.7 ± 9.6	1.1 ± 1.9	1.2 ± 5.0
C	$6.3 \pm 5.0^{**}$	5.5 ± 5.0	2.2 ± 2.3	5.0 ± 4.5
SW	$5.6 \pm 6.2^{**}$	3.8 ± 7.1	2.3 ± 4.7	2.2 ± 5.6
S	$4.0 \pm 1.6^{**}$	$5.3 \pm 3.3^*$	1.2 ± 1.2	1.3 ± 3.1
All data	$5.3 \pm 5.7^{**}$	$4.8 \pm 7.3^*$	$1.9 \pm 3.5^*$	1.9 ± 5.9

*Significant at $p \leq 0.05$. **Significant at $p \leq 0.01$.

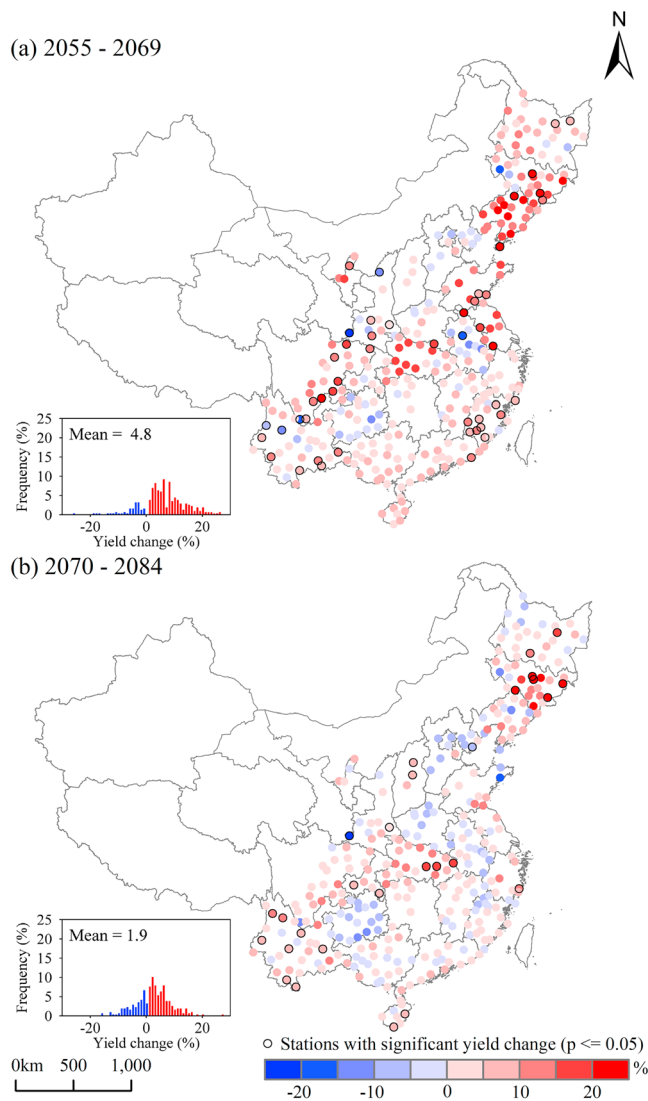


Figure 10. Rainfed rice yield differences in 318 stations between the G4 and Representative Concentration Pathway 4.5 (G4 minus Representative Concentration Pathway 4.5) averaged over the six climate models during the geoengineering phase (a) and the termination phase (b).

reported to have great impacts on rice yield in the whole China, only relative high contributions to rice yield changes can be found in the northwestern (20.9%) and eastern (44.1%) regions but not statistically significant (Table 5). However, it is worth noting that relative humidity show relatively high contribution to rice yield changes in northern China, with a contribution of 30.7%, 26.6%, and 45.8% in the northeastern, northern, and northwestern regions, respectively.

4. Discussion

4.1. Irrigated Rice Yield Change Under the Sulfate Geoengineering Scenario

The implementation of sulfate geoengineering could bring significant yield increases to rice under sufficient water supply in China, no matter during the geoengineering implementation or after the termination, which is generally in good agreement with the result of Pongratz et al. (2012) based on the implementation of sulfate geoengineering in a $2 \times \text{CO}_2$ scenario. With the implementation of sulfate geoengineering, irrigated rice yield under the G4 scenario benefits from the cooling effect and thus is higher than that under the RCP4.5 scenario, the cooling effect lasts 6 years after the termination of sulfate geoengineering (Figures 3a and 3b), bringing yield increases in most places in China.

However, the spatial distribution of the irrigated rice yield change shows that, unlike the previous findings in Pongratz et al. (2012) and Xia et al. (2014) considering the water-related effects, the implementation of sulfate geoengineering results in a pervasive yield increase both during the geoengineering phase or the termination phase, and no adverse effect from sulfate geoengineering was found in the north of China, which is because the adverse effect from precipitation is balanced by sufficient irrigation, and the dominated temperature changes brings yield increases in most of the stations in China. It was also found that the yield increase in the south part of China are weaker than that in the north areas. This can be explained that yield changes between G4 and RCP4.5 of some of the stations in the south are dominated by solar radiation (Table 4), and the decreased solar radiation in these areas partially balances the positive effect to yield change from temperature. Interestingly, the sulfur injected into the stratosphere may not be the only reason that cause this solar radiation reduction in the south of China. It was reported that sulfur can have some indirect impact on cloud and reflects more radiation (McCoy & Hartmann, 2015), and it was found that cloud cover in the south of China in G4 is significant higher than that in RCP4.5 (supporting information Figure S1), indicating it may be an important factor causing radiation reduction in southern China.

Under the sulfate geoengineering scenario, irrigated rice yield in China during 2055–2084 was found to increases compared with the current level, which is in good agreement with the result of Pongratz et al. (2012) that rice yield benefits from the combined effect of climate change and CO_2 fertilization effect. However, in our study, the irrigated rice yield in RCP4.5 is a little lower than the current level, which is in contrast with the previous findings that elevated CO_2 concentration and solar radiation in RCP4.5 leading to increased rice yield from current level (Yang et al., 2015; Zhang et al., 2019). It can be explained that the current yield level in our study was simulated based on a smooth weather change (30-year average), which provides a weather change without heat and water stress, and thus leading to higher yield than actual situation. Besides, the climate simulations we used are daily simulations, and we did not average the ensemble members for each climate model, so inevitably, there will be some weather noises (such as short-term heat stress) that eventually lead to yield losses.

Table 4
Dependence of Irrigated Rice Yield Change on Each Climate Factor

Subregion	Dependence of rice yield on climate factors (%)			Goodness of fitting (R^2)
	MaxT	MinT	SR	
NE	58.5*	33.5	8.0	0.39
N	70.6	24.0	5.4	0.53
NW	48.1	42.8	9.0	0.04
E	52.9	37.4	9.7	0.33
C	59.4	6.3	34.3	0.53
SW	54.5*	30.3	15.2	0.34
S	41.3	14.4	44.3	0.43
All data	53.6**	30.0*	16.4*	0.68

Note. The dependence is measured using the absolute value of the coefficient of each climate factor in the multiple linear regression, and the values were further converted into percentages to represent the relative contribution of each climate factor to the yield change. MaxT = maximum temperature; MinT = minimum temperature; SR = solar radiation.

*Significant at $p \leq 0.05$. **Significant at $p \leq 0.01$.

4.2. Rainfed Rice Yield Change Under the Sulfate Geoengineering Scenario

The implementation of sulfate geoengineering could lead to yield increases for rainfed rice in most areas in China, which is totally different from previous findings that the implementation could lead to rice yield losses in the high-latitude areas in China (Pongratz et al., 2012; Xia et al., 2014). The precipitation reduction cause by sulfate geoengineering is found only significant in the northeastern region in China, but the rice yield change in this region is more dominated by the temperatures, so the rice yield benefits from the prevalent cooling effect (Figures 5 and 6 and Table 4). Significant precipitation reduction can be found in both northern and southern areas in China during the termination phase, and the northern areas are more affected by this precipitation reduction, which can be explained that the northeastern China are more vulnerable to drought (Piao et al., 2010), and thus precipitation decreases have greater impacts in this area. Although precipitation is not found to have significant impact on the average rice yield in China, there is still some differences between the spatial patterns of irrigated rice yield change and rainfed rice yield change, especially in the north and central areas in

China. This may be because rainfed rice yield changes of some stations in northern and central China are dominated by relative humidity or precipitation, as these two water-related variables have a relative high contribution to rainfed rice yield change in these areas in China (Table 5). Besides, precipitation changes are often accompanied by radiation and temperature changes, and it may have some indirect impact on rice yield by affecting other climate variables.

Interestingly, after the irrigation function is turned off (rainfed yield), notwithstanding the radiation and CO₂ concentration increases, both G4 and RCP4.5 yields are lower than the current level, which can be explained that rice is more vulnerable to climate change under water stress (Doorenbos & Kassam, 1979), the fluctuations in climates can lead to greater yield loss under this circumstance, which also explains why the magnitudes of rainfed rice yield change are larger than that of irrigated rice yield change.

4.3. Uncertainties

This study focuses only on one scenario of sulfate geoengineering (G4). However, different geoengineering scenarios could bring different climate responses due to different scenario settings (Kravitz et al., 2011; Niemeier et al., 2013). Therefore, using only one scenario may not be able to fully represent the climate change of sulfate geoengineering, and various scenarios should be considered in the future studies.

Table 5
Dependence of Rainfed Rice Yield Change on Each Climate Factor

Subregion	Dependence of rice yield on climate factors (%)						Goodness of fitting (R^2)
	MaxT	MinT	SR	P	RH	WS	
NE	34.3	19.3	13.3	1.4	30.7	1.1	0.28
N	5.9	14.7	22.3	16.7	26.6	13.8	0.35
NW	0.8	1.6	19.7	20.9	45.8	11.1	0.15
E	21.4	12.5	11.0	44.1	4.5	6.5	0.35
C	31.9	25.0	23.2	3.1	16.2	0.8	0.34
SW	31.5	17.9	15.4	9.6	17.9	7.7	0.28
S	46.8**	33.1**	16.2*	2.4	1.1	0.4	0.57
All data	41.3	31.8	13.8	4.9	7.3	0.9	0.63

Note. The dependence is measured using the absolute value of the coefficient of each climate factor in the multiple linear regression, and the values were further converted into percentages to represent the relative contribution of each climate factor to the yield change. MaxT = maximum temperature; MinT = minimum temperature; SR = solar radiation; P = precipitation; RH = relative humidity; WS = wind speed.

*Significant at $p \leq 0.05$. **Significant at $p \leq 0.01$.

Moreover, new climate model experiments in GeoMIP phase 6, such as G6sulfur and G6solar (Kravitz et al., 2015), should also be considered in the future studies.

In this study, we used each ensemble member from each climate model to force the crop model; in this way, the weather variations in each ensemble member are preserved. However, there also may be some weather noises in each ensemble member, and this climate noise (such as temperature, the variation of which may exceed 20 °C during a week; Figure S2) may lead to crop failure or great yield loss and finally lead to some uncertainties. Using the average of the ensemble members can reduce these climate noises but may eliminate the weather variations in each ensemble member (Figure S2); a full comparison is required in the future study.

In this study, both irrigated and rainfed conditions were considered for future simulations, but none of them are consistent with the current background of rice cultivation in China. However, considering more and more large water conservancy projects (e.g., the South-North Water Transfer Project) being carried out in China (Liu et al., 2013) and taking into account the scientific and technological development in the future (such as the advance in irrigation water delivery efficiency, which is relatively low in China compared with the developed countries, and new rice cultivars), setting water stress to 0 (with unlimited irrigation) may be more in agreement with the condition of irrigation in China in the future. However, there still may be some factors affecting irrigation in the future such as water availability, but a full assessment of water availability is beyond the scope of this study. Therefore, addressing rainfed conditions can provide more information about insufficient irrigation that irrigated yield ignores.

Our simulations did not take into consideration the diffuse radiation because the lack of climate outputs and observation data. However, previous studies have suggested that the sulfate geoengineering can lead to more diffuse radiation (Robock et al., 2009; Xia et al., 2016) and thus promote the vegetation productivity. Therefore, this may lead to an underestimation of the rice yield under the G4 scenario and, moreover, an underestimation of dependence of rice yield on radiation.

Simulations from the crop model showed that there is a certain spatial heterogeneity of rice yield change no matter during the implementation of sulfate geoengineering or after the termination of sulfate geoengineering, even with opposite directions of yield change in the same province. This indicated that if simulations are carried out only at the provincial scale (i.e., one meteorological station for one province), the result may be not accurate to describe the rice yield change. Although 318 stations were taken into account in this study, which can represent the climate varieties in a province to a certain extent, it still cannot precisely describe the climate background of rice cultivation. Therefore, further studies should take more stations into account when the data are available. This heterogeneous yield changes also imply that the spatial resolution of the outputs from the climate model is still too coarse to simulate rice yield, and climate simulations with a higher spatial resolution are needed to accurately evaluate the impacts of geoengineering on agriculture.

We used a simple MLR to analyze the dominant climate factors that affect the rice yield. However, the rice yield simulation is quite nonlinear, and the climate factors in consideration are annual climates. Therefore, some combined effect and short-term weather events may not be captured by the linear regression model, and this can lead to some uncertainties.

5. Conclusions

In this study, climate simulations from six climate models and observations from 318 stations were combined and input into the ORYZA(v3) model to evaluate the impacts of sulfate geoengineering on rice yield in China, as well as the dependence of rice yield change on each climate factor. The results showed that the average rice yield in China increases after G4 sulfate geoengineering is implemented under both irrigated ($5.3 \pm 5.7\%$) and rainfed ($4.8 \pm 7.3\%$) conditions, and after the termination of sulfate geoengineering, the rice yield is still higher in G4 relative to RCP4.5 (only significant for irrigated yield). These results indicate that the rice in China can benefit from the implementation of sulfate geoengineering and even after the termination. But the increasing rate decreases after the termination of sulfate geoengineering. Maximum temperature is always the dominant factor affecting the rice yield change in China no matter under irrigated or rainfed conditions. However, the changes in radiation have a great effect rice yield in southern China and weaken the yield increase from cooling effect in this area. Precipitation changes was not found to have

significant impacts on average rice yield change in China under the sulfate geoengineering scenario, but precipitation and relative humidity were found to have a certain impact on rainfed rice yield change in northern and central China.

Acknowledgments

This work was supported by the National Basic Research Program of China (grant 2015CB953603), the State Key Laboratory of Earth Surface Processes and Resource Ecology (grant 2017-FX-01(1)) and the National Natural Science Foundation of China (grant 41661144006). We thank GeoMIP and all the participants of the GeoMIP who provide the climate model simulations; we also thank the Earth System Grid Federation (ESGF) and scientists managing the ESGF nodes who make the GeoMIP data available. We would like to thank the editor and two anonymous reviewers for the comments they provided to improve the quality of this paper. The climate observations can be freely downloaded from China Meteorological Data Service Center (<http://data.cma.cn/>), and the rice management data are available from Tianyi Zhang upon a reasonable request. The rice yield simulations in this study are available at Zenodo (<http://doi.org/10.5281/zenodo.2591208>).

References

- Allan, R. P., & Soden, B. J. (2008). Atmospheric warming and the amplification of precipitation extremes. *Science*, *321*(5895), 1481–1484. <https://doi.org/10.1126/science.1160787>
- Alley, R. B., Clark, P. U., Huybrechts, P., & Joughin, I. (2005). Ice-sheet and sea-level changes. *Science*, *310*(5747), 456–460. <https://doi.org/10.1126/science.1114613>
- Angstrom, A. (1924). Solar and terrestrial radiation. Report to the international commission for solar research on actinometric investigations of solar and atmospheric radiation. *Quarterly Journal of the Royal Meteorological Society*, *50*(210), 121–126. <https://doi.org/10.1002/qj.49705021008>
- Bouman, B. A. M., & van Laar, H. H. (2006). Description and evaluation of the rice growth model ORYZA2000 under nitrogen-limited conditions. *Agricultural Systems*, *87*(3), 249–273. <https://doi.org/10.1016/j.agsy.2004.09.011>
- Chylek, P., Li, J., Dubey, M. K., Wang, M., & Lesins, G. (2011). Observed and model simulated 20th century Arctic temperature variability: Canadian earth system model CanESM2. *Atmospheric Chemistry and Physics Discussions*, *11*(8), 22,893–22,907. <https://doi.org/10.5194/acpd-11-22893-2011>
- Collins, W. J., Bellouin, N., Doutriaux-Boucher, M., Gedney, N., Halloran, P., Hinton, T., et al. (2011). Development and evaluation of an Earth-System model—HadGEM2. *Geoscientific Model Development*, *4*(4), 1051–1075. <https://doi.org/10.5194/gmd-4-1051-2011>
- Crutzen, P. J. (2006). Albedo enhancement by stratospheric sulfur injections: A contribution to resolve a policy dilemma? *Climatic Change*, *77*(3–4), 211–220. <https://doi.org/10.1007/s10584-006-9101-y>
- Doorenbos, J., & Kassam, A. (1979). *Yield response to water. Irrigation and drainage paper* (Vol. 33, p. 257). Rome: FAO.
- Fischer, E. M., & Knutti, R. (2015). Anthropogenic contribution to global occurrence of heavy-precipitation and high-temperature extremes. *Nature Climate Change*, *5*(6), 560–564. <https://doi.org/10.1038/nclimate2617>
- Gregory, J. M., Huybrechts, P., & Raper, S. C. B. (2004). Climatology: Threatened loss of the Greenland ice-sheet. *Nature*, *428*(6983), 616–616. <https://doi.org/10.1038/428616a>
- Hawkins, E., Osborne, T. M., Ho, C. K., & Challinor, A. J. (2013). Calibration and bias correction of climate projections for crop modeling: An idealized case study over Europe. *Agricultural and Forest Meteorology*, *170*, 19–31. <https://doi.org/10.1016/j.agrformet.2012.04.007>
- Ji, D., Wang, L., Feng, J., Wu, Q., Cheng, H., Zhang, Q., et al. (2014). Description and basic evaluation of Beijing Normal University Earth System Model (BNU-ESM) version 1. *Geoscientific Model Development*, *7*(5), 2039–2064. <https://doi.org/10.5194/gmd-7-2039-2014>
- Keith, D. W. (2000). Geoengineering the climate: History and prospect. *Annual review of energy and the environment*, *25*(1), 245–284. <https://doi.org/10.1017/cbo9780511536038.010>
- Kravitz, B., Robock, A., Boucher, O., Schmidt, H., Taylor, K. E., Stenchikov, G., & Schulz, M. (2011). The geoengineering model inter-comparison project (GeoMIP). *Atmospheric Science Letters*, *12*(2), 162–167. <https://doi.org/10.1002/asl.316>
- Kravitz, B., Robock, A., Tilmes, S., Boucher, O., English, J. M., Irvine, P. J., et al. (2015). The geoengineering model intercomparison project phase 6 (GeoMIP6): Simulation design and preliminary results. *Geoscientific Model Development*, *8*(10), 3379–3392. <https://doi.org/10.5194/gmd-8-3379-2015>
- Lenton, T. M., & Vaughan, N. E. (2009). The radiative forcing potential of different climate geoengineering options. *Atmospheric Chemistry and Physics*, *9*(15), 5539–5561. <https://doi.org/10.5194/acp-9-5539-2009>
- Li, T., Angeles, O., Marcaida, M., Manalo, E., Manalili, M. P., Radanielson, A., & Mohanty, S. (2017). From ORYZA2000 to ORYZA (v3): An improved simulation model for rice in drought and nitrogen-deficient environments. *Agricultural and Forest Meteorology*, *237*–*238*, 246–256. <https://doi.org/10.1016/j.agrformet.2017.02.025>
- Liu, J., Zang, C., Tian, S., Liu, J., Yang, H., Jia, S., et al. (2013). Water conservancy projects in China: Achievements, challenges and way forward. *Global Environmental Change*, *23*(3), 633–643. <https://doi.org/10.1016/j.gloenvcha.2013.02.002>
- Maclean, J., Hardy, B., & Hettel, G. (2013). *Rice almanac* (4th ed.). Los Baños, Philippines: International Rice Research Institute.
- Marcaida, M. III, Li, T., Angeles, O., Evangelista, G. K., Fontanilla, M. A., Xu, J., et al. (2014). Biomass accumulation and partitioning of newly developed Green Super Rice (GSR) cultivars under drought stress during the reproductive stage. *Field Crops Research*, *162*, 30–38. <https://doi.org/10.1016/j.fcr.2014.03.013>
- Marchetti, C. (1977). On geoengineering and the CO₂ problem. *Climatic change*, *1*(1), 59–68. <https://doi.org/10.1007/bf00162777>
- Matala, J., Hynynen, J., Miina, J., Ojansuu, R., Peltola, H., Sievänen, R., et al. (2003). Comparison of a physiological model and a statistical model for prediction of growth and yield in boreal forests. *Ecological Modeling*, *161*(1–2), 95–116. [https://doi.org/10.1016/S0304-3800\(02\)00297-1](https://doi.org/10.1016/S0304-3800(02)00297-1)
- McCarty, J. P. (2001). Ecological consequences of recent climate change. *Conservation Biology*, *15*(2), 320–331. <https://doi.org/10.1046/j.1523-1739.2001.015002320.x>
- McCoy, D. T., & Hartmann, D. L. (2015). Observations of a substantial cloud-aerosol indirect effect during the 2014–2015 Bárðarbunga-VEIðivötn fissure eruption in Iceland. *Geophysical Research Letters*, *42*, 10,409–10,414. <https://doi.org/10.1002/2015GL067070>
- Meinshausen, M., Smith, S. J., Calvin, K., Daniel, J. S., Kainuma, M. L. T., Lamarque, J.-F., et al. (2011). The RCP greenhouse gas concentrations and their extensions from 1765 to 2300. *Climatic Change*, *109*(1–2), 213–241. <https://doi.org/10.1007/s10584-011-0156-z>
- Murray, F. W. (1967). On the computation of saturation vapor pressure. *Journal of Applied Meteorology*, *6*(1), 203–204. [http://doi.org/10.1175/1520-0450\(1967\)006<0203:Otcosv>2.0.Co;2](http://doi.org/10.1175/1520-0450(1967)006<0203:Otcosv>2.0.Co;2)
- Niemeier, U., Schmidt, H., Alterskjær, K., & Kristjánsson, J. (2013). Solar irradiance reduction via climate engineering: Impact of different techniques on the energy balance and the hydrological cycle. *Journal of Geophysical Research: Atmospheres*, *118*, 11,905–11,917. <https://doi.org/10.1002/2013JD020445>
- Parkes, B., Challinor, A., & Nicklin, K. (2015). Crop failure rates in a geoengineered climate: impact of climate change and marine cloud brightening. *Environmental Research Letters*, *10*(8). <https://doi.org/10.1088/1748-9326/10/8/084003>
- Patz, J. A., Campbell-Lendrum, D., Holloway, T., & Foley, J. A. (2005). Impact of regional climate change on human health. *Nature*, *438*(7066), 310–317. <https://doi.org/10.1038/nature04188>
- Phipps, S. J., Rotstayn, L. D., Gordon, H. B., Roberts, J. L., Hirst, A. C., & Budd, W. F. (2011). The CSIRO Mk3L climate system model version 1.0—Part 1: Description and evaluation. *Geoscientific Model Development*, *4*(2), 483–509. <https://doi.org/10.5194/gmd-4-483-2011>

- Piao, S., Ciais, P., Huang, Y., Shen, Z., Peng, S., Li, J., et al. (2010). The impacts of climate change on water resources and agriculture in China. *Nature*, *467*(7311), 43–51. <https://doi.org/10.1038/nature09364>
- Pongratz, J., Lobell, D. B., Cao, L., & Caldeira, K. (2012). Crop yields in a geoengineered climate. *Nature Climate Change*, *2*(2), 101–105. <https://doi.org/10.1038/nclimate1373>
- Robock, A., Marquardt, A., Kravitz, B., & Stenchikov, G. (2009). Benefits, risks, and costs of stratospheric geoengineering. *Geophysical Research Letters*, *36*, L19703. <https://doi.org/10.1029/2009GL039209>
- Robock, A., Oman, L., & Stenchikov, G. L. (2008). Regional climate responses to geoengineering with tropical and Arctic SO₂ injections. *Journal of Geophysical Research*, *113*, D16101. <https://doi.org/10.1029/2008JD010050>
- Rosenzweig, C., & Parry, M. L. (1994). Potential impact of climate change on world food supply. *Nature*, *367*(6459), 133–138. <https://doi.org/10.1038/367133a0>
- Stocker, T., Qin, D., Plattner, G., Tignor, M., Allen, S., Boschung, J., et al. (2013). *IPCC, 2013: Summary for policymakers. Climate change 2013: The physical science basis. Contribution of working group I to the fifth assessment report of the intergovernmental panel on climate change*. Cambridge, UK and New York: Cambridge University Press.
- Walther, G.-R., Post, E., Convey, P., Menzel, A., Parmesan, C., Beebee, T. J. C., et al. (2002). Ecological responses to recent climate change. *Nature*, *416*(6879), 389–395. <https://doi.org/10.1038/416389a>
- Watanabe, S., Hajima, T., Sudo, K., Nagashima, T., Takemura, T., Okajima, H., et al. (2011). MIROC-ESM 2010: Model description and basic results of CMIP5-20c3m experiments. *Geoscientific Model Development*, *4*(4), 845–872. <https://doi.org/10.5194/gmd-4-845-2011>
- Xia, L., Robock, A., Cole, J., Curry, C. L., Ji, D., Jones, A., et al. (2014). Solar radiation management impacts on agriculture in China: A case study in the Geoengineering Model Intercomparison Project (GeoMIP). *Journal of Geophysical Research: Atmospheres*, *119*, 8695–8711. <https://doi.org/10.1002/2013JD020630>
- Xia, L., Robock, A., Tilmes, S., & Neely III, R. R. (2016). Stratospheric sulfate geoengineering could enhance the terrestrial photosynthesis rate. *Atmospheric Chemistry and Physics*, *16*(3), 1479–1489. <https://doi.org/10.5194/acp-16-1479-2016>
- Yadav, S., Li, T., Humphreys, E., Gill, G., & Kukal, S. S. (2011). Evaluation and application of ORYZA2000 for irrigation scheduling of puddled transplanted rice in north west India. *Field Crops Research*, *122*(2), 104–117. <https://doi.org/10.1016/j.fcr.2011.03.004>
- Yang, X., Chen, F., Lin, X., Liu, Z., Zhang, H., Zhao, J., et al. (2015). Potential benefits of climate change for crop productivity in China. *Agricultural and Forest Meteorology*, *208*, 76–84. <https://doi.org/10.1016/j.agrformet.2015.04.024>
- Zhang, H., Zhou, G., Li Liu, D., Wang, B., Xiao, D., & He, L. (2019). Climate-associated rice yield change in the Northeast China Plain: A simulation analysis based on CMIP5 multi-model ensemble projection. *Science of the Total Environment*, *666*, 126–138. <https://doi.org/10.1016/j.scitotenv.2019.01.415>
- Zhang, T., Yang, X., Wang, H., Li, Y., & Ye, Q. (2014). Climatic and technological ceilings for Chinese rice stagnation based on yield gaps and yield trend pattern analysis. *Global Change Biology*, *20*(4), 1289–1298. <https://doi.org/10.1111/gcb.12428>